PSF1 are required for maintenance of pool size of immature hematopoietic cells and acute bone marrow regeneration. Blood 2009; 113:555–62.
15. Obama K, Ura K, Satoh S, Nakamura Y, Furukawa Y. Up-regulation of PSF2, a member of the GINS multiprotein complex, in intrahepatic cholangiocarcinoma. Oncol Rep 2005;14:701–6.
16. Hayashi R, Arauchi T, Tategu M, Goto Y, Yoshida K. A combined computational and experimental study on the structure-regulation relationships of putative mammalian DNA replication initiator GINS. Genomics Proteomics Bioinformatics 2006;4:156–64.
17. Ryu B, Kim DS, Deluca AM, Alani RM. Comprehensive expression profiling of tumor cell lines identifies molecular signatures of melanoma progression. PLoS One 2007;2:e594.
18. Ben-Porath I, Thomson MW, Carey VJ, et al. An embryonic stem cell-like gene expression signature in poorly differentiated aggressive human tumors. Nat Genet 2008;40:499–507.
19. Satoh N, Yamada Y, Kinugasa Y, Takakura N. Angiopoietin-1 alters tumor growth by stabilizing blood vessels or by promoting angiogenesis. Cancer Sci 2008;99:2373–9.
20. Kanda T, Sullivan KF, Wahl GM. Histone-GFP fusion protein enables sensitive analysis of chromosome dynamics in living mammalian cells. Curr Biol 1998;8:377–85.
21. Fujita H, Fukuhara S, Sakurai A, et al. Local activation of Rap1 contributes to directional vascular endothelial cell migration accompanied by extension of microtubules on which RAPL, a Rap1-associating molecule, localizes. J Biol Chem 2005;280:5022–31.
22. Fukuhara S, Sako K, Minami T, et al. Differential function of Tie2 at cell-cell contacts and cell-substratum contacts regulated by angiopoietin-1. Nat Cell Biol 2008;10:513–26.
23. Subramanian A, Tamayo P, Mootha VK, et al. Gene set enrichment analysis: a knowledge-based approach for interpreting genome-wide expression profiles. Proc Natl Acad Sci U S A 2005;102:15545–50.
24. Wong DJ, Liu H, Ridky TW, Cassarino D, Segal E, Chang HY. Module map of stem cell genes guides creation of epithelial cancer stem cells. Cell Stem Cell 2008;2:333–44.
25. Somervaille TC, Matheny CJ, Spencer GJ, et al. Hierarchical maintenance of MLL myeloid leukemia stem cells employs a transcriptional program shared with embryonic rather than adult stem cells. Cell Stem Cell 2009;4:129–40.
26. Calabrese C, Poppleton H, Kocak M, et al. A perivascular niche for brain tumor stem cells. Cancer Cell 2007;11:69–82.
27. Kiel MJ, Yilmaz OH, Iwashita T, Terhorst C, Morrison SJ. SLAM family receptors distinguish hematopoietic stem and progenitor cells and reveal endothelial niches for stem cells. Cell 2005;121:1109–21.
28. Tozer GM, Kanthou C, Baguley BC. Disrupting tumour blood vessels. Nat Rev Cancer 2005;5:423–35.
29. Paez-Ribes M, Allen E, Hudock J, et al. Antiangiogenic therapy elicits malignant progression of tumors to increased local invasion and distant metastasis. Cancer Cell 2009;15:220–31.
30. Okamoto R, Ueno M, Yamada Y, et al. Hematopoietic cells regulate the angiogenic switch during tumorigenesis. Blood 2005;105: 2757–63.
31. Kearsey SE, Cotterill S. Enigmatic variations: divergent modes of regulating eukaryotic DNA replication. Mol Cell 2003;12:1067–75.
32. Hemerly AS, Prasanth SG, Siddiqui K, Stillman B. Orc1 controls centriole and centrosome copy number in human cells. Science 2009; 323:789–93.
33. Prasanth SG, Prasanth KV, Stillman B. Orc6 involved in DNA replication, chromosome segregation, and cytokinesis. Science 2002;297: 1026–31.

Biochemical and Biophysical Research Communications 392 (2010) 150–154

Contents lists available at ScienceDirect

Biochemical and Biophysical Research Communications

journal homepage: www.elsevier.com/locate/ybbrc

PSF3 marks malignant colon cancer and has a role in cancer cell proliferation

Yumi Nagahama [a], Masaya Ueno [a,b], Naotsugu Haraguchi [c], Masaki Mori [c], Nobuyuki Takakura [a,*]

[a] Department of Signal Transduction, Research Institute for Microbial Diseases, Osaka University, 3-1 Yamadaoka, Suita, Osaka 565-0871, Japan
[b] Department of Molecular, Cell and Developmental Biology, University of California, Los Angeles, CA 90095, USA
[c] Department of Gastroenterological Surgery, Graduate School of Medicine, Osaka University, 2-2 Yamadaoka, Suita, 565-0871, Japan

ARTICLE INFO

Article history:
Received 22 December 2009
Available online 6 January 2010

Keywords:
PSF3
Colon carcinoma

ABSTRACT

PSF3 (partner of Sld five 3) is a member of the tetrameric complex termed GINS, composed of SLD5, PSF1, PSF2, and PSF3, and well-conserved evolutionarily. Previous studies suggested that some GINS complex members are upregulated in cancer, but PSF3 expression in colon carcinoma has not been investigated. Here, we established a mouse anti-PSF3 antibody, and examined PSF3 expression in human colon carcinoma cell lines and colon carcinoma specimens. We found that PSF3 is expressed in the crypt region in normal colonic mucosa and that many PSF3-positive cells co-expressed Ki-67. This suggests that PSF3-positivity of normal mucosa is associated with cell proliferation. Expression of the PSF3 protein was greater in carcinoma compared with the adjacent normal mucosa, and even stronger in high-grade malignancies, suggesting that it may be associated with colon cancer progression. PSF3 gene knock-down in human colon carcinoma cell lines resulted in growth inhibition characterized by delayed S-phase progression. These results suggest that PSF3 is a potential biomarker for diagnosis of progression in colon cancer and could be a new target for cancer therapy.

Introduction

PSF3 (partner of Sld five 3) is a member of the highly evolutionarily conserved tetrameric complex termed GINS, composed of SLD5, PSF1, PSF2, and PSF3. In yeast, the GINS complex associates with the Minichromosome maintenance (MCM) 2–7 complex and with CDC45, and this "C-M-G complex" (CDC45-MCM-2-7-GINS) regulates both the initiation and progression of DNA replication [1–6]. Thus, it has been suggested that GINS is involved in DNA replication in *Xenopus* and human [7–10]. However, a recent study suggested that PSF1/2 is associated with the response to replication stress and acquisition of DNA damage in untransformed human dermal fibroblasts [11]. As it has been reported that DNA replication-associated protein in yeast has diverse functions in different cells, e.g. origin recognition protein Orc1 has a role in determining centrosome copy number [12], the exact functions of GINS components in mammalian cells are not yet clear.

We have previously cloned the mouse ortholog of *PSF1* (partner of SLD5) from a hematopoietic stem cell (HSC) cDNA library [13] and found that *PSF1* expression in mice was predominantly observed in the adult BM and thymus, as well as the testis and ovary, i.e. tissues in which stem cell proliferation is actively induced and continues after birth. Moreover, we reported that PSF1 is strongly expressed in several immature cell lineages such as cells in the inner cell mass during early embryogenesis, and spermatogonia as well as HSCs after birth [13–15]. Loss of *PSF1* led to embryonic lethality around the implantation stage caused by the inability of cells of the inner cell mass to proliferate [13]. Moreover, haploinsufficiency of PSF1 in $PSF1^{+/-}$ mice resulted in the delayed induction of HSC proliferation during reconstitution of bone marrow after 5-FU ablation. These data strongly suggested that PSF1 is required for acute proliferation of cells, especially immature cells such as stem cells and progenitor cells. However, the role of the other components of GINS in mammalian cells has not been well determined.

Several recent reports have suggested a role for GINS components in cancer cells. For example, all GINS components were found to be overexpressed in intrahepatic cholangiocarcinoma tissues [16]. In a Gene Expression Omnibus (GEO) database search, *PSF1* was identified as an estrogen target in MCF7 human breast carcinoma cells [17]. In a comprehensive study, it was found that *PSF1* and *SLD5* were upregulated in aggressive melanoma [18].

Although several studies have suggested that GINS components play a role in cancer as described above, their expression in colon carcinoma has not been examined. Among the GINS complex members, the expression and role of PSF3 has not been well-documented because no appropriate antibody was available thus far. Therefore, we generated such an antibody against PSF3 and

Abbreviations: GINS, Go-ichi-nii-san; PSF, Partner of Sld five.

* Corresponding author. Fax: +81 6 6879 8314.
E-mail address: ntakaku@biken.osaka-u.ac.jp (N. Takakura).

0006-291X/$ - see front matter © 2010 Elsevier Inc. All rights reserved.
doi:10.1016/j.bbrc.2009.12.174

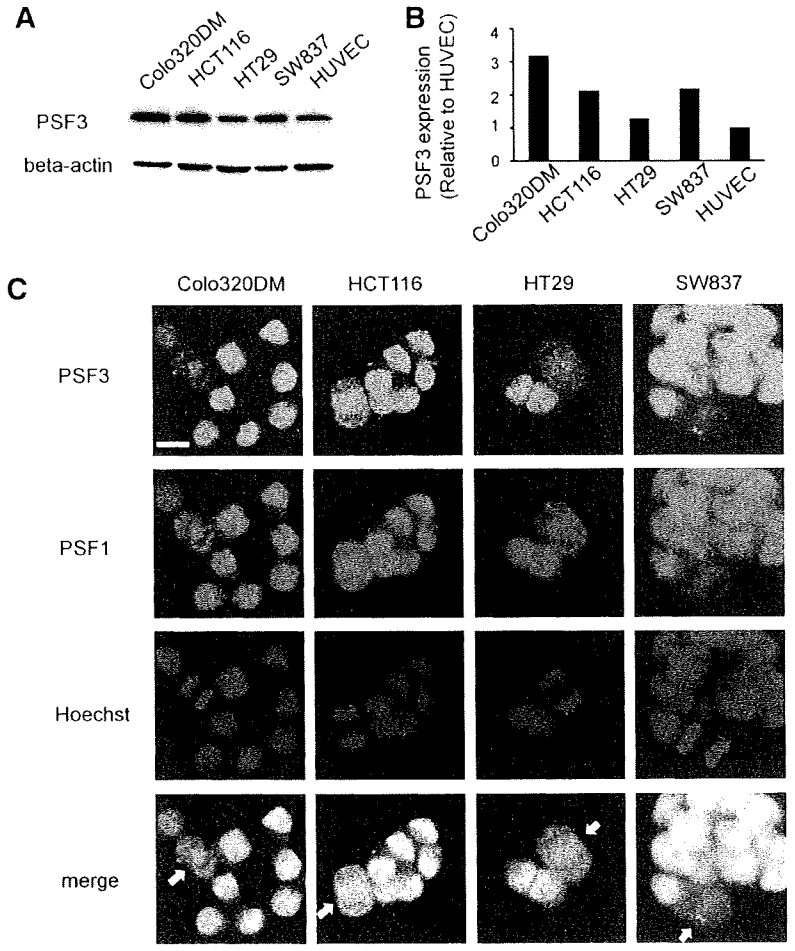

Fig. 1. PSF3 expression in human colon carcinoma cell lines. (A,B) Western blotting of PSF3 expression in whole cell extracts of each cell line as indicated. A representative result of Western blotting (A) and densitometric analysis for quantitative evaluation (B) are shown. (C) Cells as indicated were stained with anti-PSF3 antibody labeled with Alexa488 (green) and co-stained with anti-PSF1 antibody labeled with Cy3 (red). DNA was counter-stained with Hoechst (blue). Arrows, mitotic cells. Bar, 10 μm.

examined its reactivity with human colon carcinoma specimens. Furthermore, we silenced the *PSF3* gene by RNAi methodology to determine the impact of PSF3 knock-down on the growth of human colon carcinoma cell lines.

Materials and methods

Generation of anti-PSF3 antibody. For the generation of monoclonal anti-PSF3 antibody, PSF3 cDNA, coding full-length amino acid residues, was amplified by polymerase chain reaction (PCR), and then DNA fragments were ligated into pGEX-2T vector (Pharmacia Piscataway, NJ) for the preparation of glutathione *S*-transferase (GST)-fusion proteins. Purified GST-fused protein was used as antigen for mouse immunization, and hybridoma cells were established by standard procedures. Finally, stable hybridoma cell lines were obtained and cloned as aps3.2 and aps3.14. In this current study, aps3.2 was used. The specificities of the antibodies were analyzed by Western blotting and immunocytochemistry.

Cell lines. HCT116, colo320DM, SW837, HT-29 were maintained in RPMI medium (Sigma, St. Louis, MO) with 10% fetal bovine serum (FBS) (Sigma) and penicillin/streptomycin (GIBCO, Rockville, MD). Human umbilical vein endothelial cells (HUVECs) were maintained in HuMedia EG2 (Kurabo, Osaka, Japan).

Western blotting. Total cell lysates were heated for 3 min at 95 °C and then loaded onto SDS–polyacrylamide gels. Proteins were electrophoretically transferred onto polyvinylidene difluoride membranes (Millipore, MA, USA), blocked with 5% nonfat dry milk, then blotted with anti-PSF3 antibody or anti-beta actin antibody (Sigma). Blots were developed with peroxidase-labeled anti-mouse Ig antibodies (Dako, Carpinteria, CA) using enhanced chemiluminescence (ECL detection system; Amersham, Buckinghamshire, UK).

Immunocytochemistry. For staining of PSF1 and PSF3, 4% PFA in phosphate buffer saline (PBS) and cold methanol was used for fixations. Following three washes with PBS, cells were incubated with anti-PSF1 [15] and anti-PSF3 antibody, then washed with PBS and incubated with goat anti-mouse IgG Alexa488 (for PSF3, Invitrogen, Carlsbad, CA, USA) or anti-rat IgG Biotin (for PSF1, Invitrogen) followed by Streptavidin-Cy3 (Zymed). Nuclear DNA was counter-stained with Hoechst (Sigma).

Immunohistochemistry. For human specimens, immnohistochemistry was performed on formalin-fixed, paraffin-embedded tumor samples. All specimens were obtained from the Department of Gastroenterological Surgery, Graduate School of Medicine, Osaka University. For the immunohistochemical analyses, mouse anti-PSF3 antibody (aps3.2) or anti-Ki-67 antibody (Dako) was used for primary antibodies. As a secondary antibody for anti-PSF3 or anti-Ki-67 antibody, Biotin-conjugated goat anti-mouse Ig (Dako) was used. After washing the slides three times with 0.05% Triton X-100 in PBS, they are incubated with VECSTAIN ABC Standard

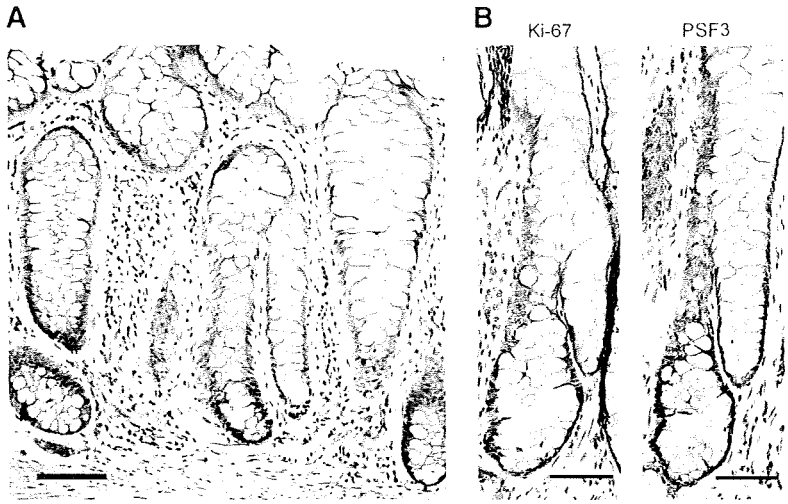

Fig. 2. PSF3 expression in human colonic mucosa. (A) Immunohistochemical analysis of PSF3 (brown) expression in human colonic mucosa. Bar, 100 μm. (B) Immunohistochemical analysis of Ki-67 (brown) and PSF3 (brown) expression in serial sections of human colon mucosa. Bars, 50 μm.

Kit (Vector Laboratories, Burlingame, CA, USA). For the visualization of HRP, diaminobenzidine (Dojindo, Kumamoto, Japan) was used. The slides were counter-stained with hematoxylin.

RNA interference. Small interfering RNA (siRNA) specific to human PSF3 and negative control siRNA were purchased from Invitrogen. The effect of siRNA transfection was optimized using RNAiMAX (Invitrogen) according to the manufacturer's protocol. The effect of siRNA on PSF3 expression was observed using Western blotting with an anti-PSF3 antibody. Cell numbers were counted by a hemocytometer.

BrdU-FACS. For BrdU detection, 10 μM BrdU was added to the medium for 15 min prior to cell collection. Cells were fixed in 70% ethanol and washed in PBS, treated with 1 N HCl for 30 min and incubated with anti-BrdU antibody (BD Bioscience Pharmingen, SanDiego, USA), followed by anti-mouse IgG Alexa488 (Invitrogen).

Results

PSF3 expression in human colon carcinoma cell lines

We compared the expression of PSF3 in human colon carcinoma cell lines and non-tumor cells (HUVECs). Overall, tumor cells expressed higher levels of PSF3 protein than HUVECs (Fig. 1A and B). Next, we performed immunocytochemistry to localize PSF3 in colon carcinoma cells. Nuclear accumulation of PSF3 was observed during interphase, whereas during mitosis, it was almost exclusively located outside the chromatin with a diffuse pattern

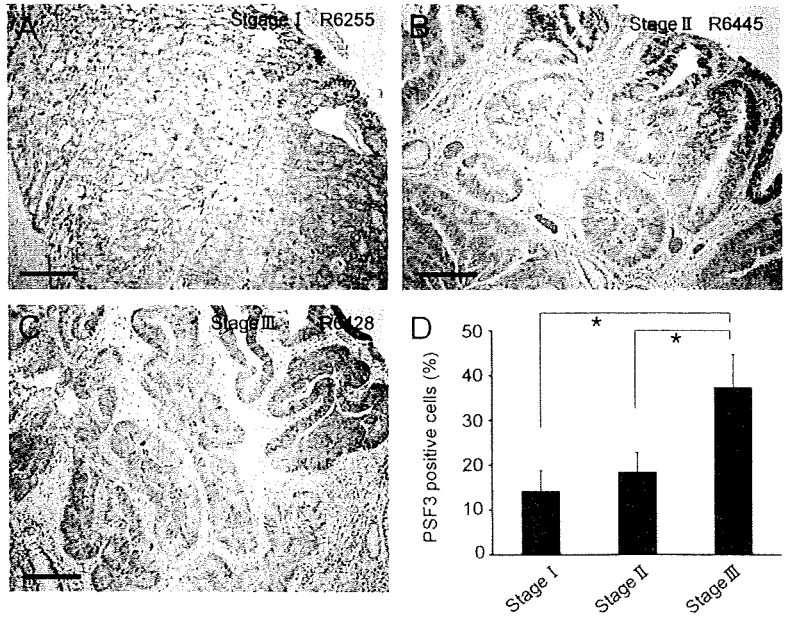

Fig. 3. PSF3 expression in human colon carcinoma specimens. (A–C) PSF3 (brown) expression in human colon carcinoma specimens in different stages (A, stage I; B, stage II; C, stage III). Bars, 200 μm. (D) Percentages of tumor cells that are PSF3-positive. $^{*}P < 0.05$ ($n = 6$, mean ± SEM).

(Fig. 1C). These characteristics are similar to PSF1, one of the other GINS components (Fig. 1C), suggesting colocalization of PSF3 and PSF1 as a GINS component in human colon carcinoma cells.

PSF3 expression in human normal colonic mucosa and colon carcinoma specimens

Several studies have suggested that GINS components play a role in tumor progression [16–18]. To test whether PSF3 may also be involved in human colon cancer progression, its expression in colon carcinoma pathological specimens was investigated using immunohistochemistry.

In adjacent normal large bowel mucosa, PSF3 expression was confined to the base of the colon crypts, which corresponds to the proliferative zone of the mucosa (Fig. 2A). Using serial tissue sections, we compared expression of PSF3 with Ki-67, a marker of proliferation. The majority of PSF3-positive cells was found to co-express Ki-67 (Fig. 2B), indicating cell cycling. Our previous study showed that PSF1 is also expressed in crypt base columnar cells and that the number of such cells decreased in adult haploinsufficient *PSF1*$^{+/-}$ mice compared with adult wild-type mice [15]. Based on these results, we suggest that the GINS complex may play an important role in proliferation of colon crypt cells.

Additionally, in colon carcinoma specimens from patients, higher levels of expression of PSF3 protein were found in the cancer cells than the adjacent normal mucosa. Moreover, the percentage of PSF3-positive cancer cells correlated positively with the stage of cancer (Fig. 3). This further suggests that PSF3 protein expression associates with colon cancer progression.

PSF3 knock-down results in growth arrest of human colon carcinoma cells

To assess whether PSF3 is involved in colon cancer cell proliferation, we evaluated the silencing effect of PSF3 on cell growth using RNAi methodology to target three different coding regions of the human *PSF3* mRNA sequence. The efficiency of *PSF3* knock-down was examined by Western blotting, indicating that PSF3 protein expression in both HCT116 and colo320DM cells was greatly attenuated, in particular by two different sequences (siPSF3-2, 3) (Fig. 4A). PSF3 knock-down in either cell line resulted in inhibition of proliferation (Fig. 4B). This inhibitory effect correlated with PSF3 expression silencing efficiency, because less effects on cell proliferation were observed with siPSF3-1. The relationship of cell cycling to reduction of PSF3 expression was assessed by the incorporation of nucleotide analogues. Results indicated that attenuation of PSF3

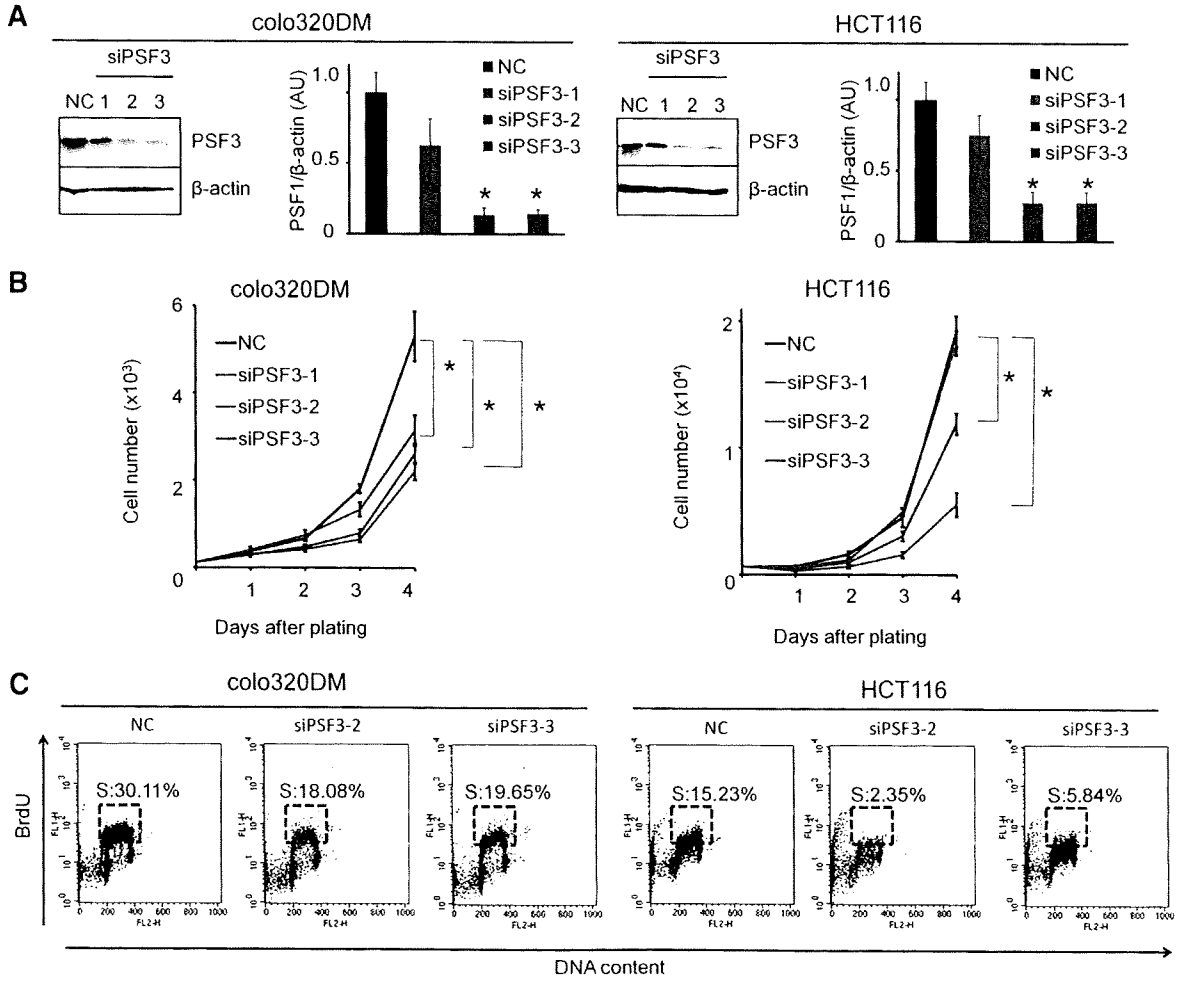

Fig. 4. PSF3 knock-down results in growth inhibition in colon carcinoma cell lines. (A) Western blotting for PSF3 expression after silencing by three RNAis (siPSF3-1, 2 and 3) or a control RNAi (NC). Densitometric analysis was performed for quantitative evaluation ($n = 4$). $^*P < 0.05$ vs control. (B) Cell growth after introduction of RNAi as described in (A). $^*P < 0.05$ ($n = 8$, mean ± SEM). (C) Cellular BrdU incorporation assay was carried out 48 h after transfection with the indicated siRNA. BrdU was incorporated for 15 min. BrdU intensity is represented in the logarithmic *y*-axis and DNA content on the linear *x*-axis. Gates define the percentage of cells in S-phase.

expression reduced the percentage of cells in S-phase (Fig. 4C). Thus, we conclude that PSF3 plays a role in cell cycling, especially S-phase progression.

Discussion

In this study, we found high levels of expression of PSF3 in several colon carcinoma cell lines and overexpression of PSF3 in stage-matched human colon cancer cells from higher grade tumors. Our preliminary experiments showed that PSF3 is more highly expressed in cancer cells invading into muscle than in non-invasive cancer (data not shown). It has been reported that several prereplicative complex proteins are overexpressed in cancer and serve as good tumor markers [19]. For example, MCM-2 (a member of the C–M–G complex) was reported to be significantly associated with Dukes' stage, existence of lymph node metastasis, tumor histological grade, presence of malignancy in adenoma, and venous invasion in colon cancer [20]. Based on these findings, our present data suggest that PSF3 might be a potential biomarker for diagnosis of progression and during the initiation of metastasis in colon cancer. Comparison of PSF3 with other proliferation markers, such as Ki-67 and PCNA, might support this hypothesis.

Previous studies have shown that DNA replication factors, including GINS, are differently expressed in *Xenopus*, suggesting that different factors are utilized in different developmental regions [21]. Further studies of precise expression profiles and functions of individual GINS components in mammalian tissues might help us to understand how such individual components are involved in tumor growth occurring in a wide variety of tissues and organs. Here, we documented PSF3 expression in the base of the crypts in normal colon and found that PSF3 expression was co-localized with PSF1 in human colon carcinoma cell lines. Moreover, PSF3 knock-down resulted in growth inhibition of colon cancer cells by the suppression of S-phase progression, indicating that PSF3 acts at least as a GINS complex and is essential for S-phase progression in human colon carcinoma cells. Further studies are required to elucidate the contributions of individual GINS components in the growth of other tumors.

Several studies have indicated that pre-RC proteins may potentially have significant therapeutic value [19]. Interestingly, Orc6, one such pre-RC protein, was reported to be associated with 5-fluorouracil (5-FU) resistance in human colon cancer cell lines [22], and its downregulation sensitized colon cancer cells to 5-FU and cisplatin [23]. These results suggest that pre-RC proteins may play a role in chemoresistance. Based on these reports, our data suggest that PSF3 might be a potential therapeutic target as well as a potential diagnosis marker for colon carcinoma.

Acknowledgments

We are grateful to N. Fujimoto and K. Fukuhara for technical assistance. This work was partly supported by the Japanese Ministry of Education, Culture, Sports, Science and Technology and the Japanese Society for Promotion of Science.

References

[1] Y. Takayama, Y. Kamimura, M. Okawa, S. Muramatsu, A. Sugino, H. Araki, GINS, a novel multiprotein complex required for chromosomal DNA replication in budding yeast, Genes Dev. 17 (2003) 1153–1165.
[2] C. Bauerschmidt, S. Pollok, E. Kremmer, H.P. Nasheuer, F. Grosse, Interactions of human Cdc45 with the Mcm2–7 complex, the GINS complex, and DNA polymerases delta and epsilon during S phase, Genes Cells 12 (2007) 745–758.
[3] A. Gambus, R.C. Jones, A. Sanchez-Diaz, et al., GINS maintains association of Cdc45 with MCM in replisome progression complexes at eukaryotic DNA replication forks, Nat. Cell Biol. 8 (2006) 358–366.
[4] M. Kanemaki, A. Sanchez-Diaz, A. Gambus, K. Labib, Functional proteomic identification of DNA replication proteins by induced proteolysis in vivo, Nature 423 (2003) 720–724.
[5] S.E. Moyer, P.W. Lewis, M.R. Botchan, Isolation of the Cdc45/Mcm2–7/GINS (CMG) complex, a candidate for the eukaryotic DNA replication fork helicase, Proc. Natl. Acad. Sci. USA 103 (2006) 10236–10241.
[6] M. Pacek, A.V. Tutter, Y. Kubota, H. Takisawa, J.C. Walter, Localization of MCM2–7, Cdc45, and GINS to the site of DNA unwinding during eukaryotic DNA replication, Mol. Cell 21 (2006) 581–587.
[7] Y.P. Chang, G. Wang, V. Bermudez, J. Hurwitz, X.S. Chen, Crystal structure of the GINS complex and functional insights into its role in DNA replication, Proc. Natl. Acad. Sci. USA 104 (2007) 12685–12690.
[8] M. De Falco, E. Ferrari, M. De Felice, M. Rossi, U. Hubscher, F.M. Pisani, The human GINS complex binds to and specifically stimulates human DNA polymerase alpha-primase, EMBO Rep. 8 (2007) 99–103.
[9] K. Kamada, Y. Kubota, T. Arata, Y. Shindo, F. Hanaoka, Structure of the human GINS complex and its assembly and functional interface in replication initiation, Nat. Struct. Mol. Biol. 14 (2007) 388–396.
[10] Y. Kubota, Y. Takase, Y. Komori, et al., A novel ring-like complex of *Xenopus* proteins essential for the initiation of DNA replication, Genes Dev. 17 (2003) 1141–1152.
[11] L.R. Barkley, I.Y. Song, Y. Zou, C. Vaziri, Reduced expression of GINS complex members induces hallmarks of pre-malignancy in primary untransformed human cells, Cell Cycle 8 (2009) 1577–1588.
[12] A.S. Hemerly, S.G. Prasanth, K. Siddiqui, B. Stillman, Orc1 controls centriole and centrosome copy number in human cells, Science 323 (2009) 789–793.
[13] M. Ueno, M. Itoh, L. Kong, K. Sugihara, M. Asano, N. Takakura, PSF1 is essential for early embryogenesis in mice, Mol. Cell. Biol. 25 (2005) 10528–10532.
[14] Y. Han, M. Ueno, Y. Nagahama, N. Takakura, Identification and characterization of stem cell-specific transcription of PSF1 in spermatogenesis, Biochem. Biophys. Res. Commun. 380 (2009) 609–613.
[15] M. Ueno, M. Itoh, K. Sugihara, M. Asano, N. Takakura, Both alleles of PSF1 are required for maintenance of pool size of immature hematopoietic cells and acute bone marrow regeneration, Blood 113 (2009) 555–562.
[16] K. Obama, K. Ura, S. Satoh, Y. Nakamura, Y. Furukawa, Up-regulation of PSF2, a member of the GINS multiprotein complex, in intrahepatic cholangiocarcinoma, Oncol. Rep. 14 (2005) 701–706.
[17] R. Hayashi, T. Arauchi, M. Tategu, Y. Goto, K. Yoshida, A combined computational and experimental study on the structure–regulation relationships of putative mammalian DNA replication initiator GINS, Genomics Proteomics Bioinformatics 4 (2006) 156–164.
[18] B. Ryu, D.S. Kim, A.M. Deluca, R.M. Alani, Comprehensive expression profiling of tumor cell lines identifies molecular signatures of melanoma progression, PLoS One 2 (2007) e594.
[19] E. Lau, T. Tsuji, L. Guo, S.H. Lu, W. Jiang, The role of pre-replicative complex (pre-RC) components in oncogenesis, FASEB J. 21 (2007) 3786–3794.
[20] C. Giaginis, M. Georgiadou, K. Dimakopoulou, et al., Clinical significance of MCM-2 and MCM-5 expression in colon cancer: association with clinicopathological parameters and tumor proliferative capacity, Dig. Dis. Sci. 54 (2009) 282–291.
[21] B.E. Walter, J.J. Henry, Embryonic expression of pre-initiation DNA replication factors in *Xenopus laevis*, Gene Expr. Patterns 5 (2004) 81–89.
[22] Y. Xi, G. Nakajima, J.C. Schmitz, E. Chu, J. Ju, Multi-level gene expression profiles affected by thymidylate synthase and 5-fluorouracil in colon cancer, BMC Genomics 7 (2006) 68.
[23] E.J. Gavin, B. Song, Y. Wang, Y. Xi, J. Ju, Reduction of Orc6 expression sensitizes human colon cancer cells to 5-fluorouracil and cisplatin, PLoS One 3 (2008) e4054.

Molecular Pharmacology Fast Forward. Published on January 22, 2010 as doi:10.1124/mol.109.061481

MOL#61481

Title page

Sphingosine 1-Phosphate Regulates Vascular Contraction via $S1P_3$ Receptor: Investigation Based on a New $S1P_3$ Receptor Antagonist

Akira Murakami, Hiroshi Takasugi, Shinya Ohnuma, Yuuki Koide, Atsuko Sakurai, Satoshi Takeda, Takeshi Hasegawa, Jun Sasamori, Takashi Konno, Kenji Hayashi, Yoshiaki Watanabe, Koji Mori, Yoshimichi Sato, Atsuo Takahashi, Naoki Mochizuki, and Nobuyuki Takakura

Tokyo Research Laboratories, Drug Research Department, TOA EIYO Ltd., Saitama, Japan (A.M., H.T., S.O., Y.K., Y.S.); Fukushima Research Laboratories, Drug Research Department, TOA EIYO Ltd., Fukushima, Japan (T.H., J.S., T.K., K.H., Y.W., K.M., A.T.); Department of Emergency Medicine, Jikei University School of Medicine, Tokyo, Japan (S.T.); Department of Structural Analysis, National Cardiovascular Center Research Institute, Osaka, Japan (A.S., N.M.); and Department of Signal Transduction, Research Institute for Microbial Diseases, Osaka University, Osaka, Japan (N.T.)

Running title page

a) Vascular Contraction Regulated by $S1P_3$ Receptor

b) Address correspondence to:

Name; Akira Murakami

Address; Drug Research Department, Tokyo Research Laboratories, TOA EIYO Ltd., 2-293-3 Amanuma, Omiya, Saitama 330-0834, Japan.

Telephone; +81-48-647-7971 Fax; +81-48-648-0078

E-mail; murakami.akira@toaeiyo.co.jp

c) 40 pages of text, 0 tables, 9 figures, 39 references

Abstract; 220 words, Introduction; 547 words, Discussion; 1152 words

d) Abbreviations:

S1P, sphingosine 1-phosphate; GPCR, G protein-coupled receptor; TY-52156, 1-(4-chlorophenylhydrazono)-1-(4-chlorophenylamino)-3,3-dimethyl-2-butanone; MAPK, mitogen-activated protein kinase; CF, coronary flow; CHO-K1, Chinese hamster ovary; HUVECs, human umbilical vein endothelial cells; HCASMCs, human coronary artery smooth muscle cells; Fura-2 AM, Fura-2 pentaacetoxymethylester; SBP, systemic blood pressure; HR, heart rate; MBP, mean blood pressure

Abstract

Sphingosine 1-phosphate (S1P) induces diverse biological responses in various tissues by activating specific G protein-coupled receptors ($S1P_1$-$S1P_5$ receptors). The biological signaling regulated by $S1P_3$ receptor has not been fully elucidated because of the lack of a $S1P_3$ receptor-specific antagonist or agonist. We developed a novel $S1P_3$ receptor antagonist, 1-(4-chlorophenylhydrazono)-1-(4-chlorophenylamino)-3,3-dimethyl-2-butanone (TY-52156), and show here that the S1P-induced decrease in coronary flow (CF) is mediated by $S1P_3$ receptor. In functional studies, TY-52156 showed sub-micromolar potency and a high degree of selectivity for $S1P_3$ receptor. TY-52156, but not an $S1P_1$ receptor antagonist (VPC23019) or $S1P_2$ receptor antagonist (JTE013), inhibited the decrease in CF induced by S1P in isolated perfused rat hearts. We further investigated the effect of TY-52156 on both the S1P-induced increase in intracellular calcium ($[Ca^{2+}]_i$) and Rho activation that are responsible for the contraction of human coronary artery smooth muscle cells. TY-52156 inhibited both the S1P-induced increase in $[Ca^{2+}]_i$ and Rho activation. In contrast, VPC23019 and JTE013 inhibited only the increase in $[Ca^{2+}]_i$ and Rho activation, respectively. We further confirmed that TY-52156 inhibited FTY-720-induced $S1P_3$ receptor-mediated bradycardia in vivo. These results clearly show that TY-52156 is both sensitive and useful as a $S1P_3$ receptor-specific antagonist, and reveal that S1P induces vasoconstriction by directly activating $S1P_3$ receptor and through a subsequent increase in $[Ca^{2+}]_i$ and Rho activation in vascular smooth muscle cells.

Introduction

Sphingosine 1-phosphate (S1P) is a bioactive lysophospholipid mediator that is mainly released from activated platelets and induces many biological responses, including angiogenesis, vascular development and cardiovascular function (Siess, 2002; Takuwa et al., 2008; Yatomi, 2006). A wide variety of biological cellular responses to S1P have been ascribed to the presence of five S1P receptors, $S1P_1$-$S1P_5$ receptors, that belong to the family of G protein-coupled receptors (GPCRs). Furthermore, a variation of heterotrimeric G protein downstream of S1P receptors accounts for the diversity of cellular responses to S1P (Rosen et al., 2009). In addition to the coupling of S1P receptors and G proteins, the expression of the combination of S1P receptors determines multiple cellular responses. To identify the signaling that is specific for each receptor, S1P receptor antagonists have been developed and have contributed to our understanding of S1P-mediated signaling (Huwiler and Pfeilschifter, 2008).

$S1P_1$-$S1P_5$ receptors couple to different G proteins upon binding to S1P. While, $S1P_1$, $S1P_4$ and $S1P_5$ receptors mainly couple to Gi, $S1P_2$ and $S1P_3$ receptors couple to Gi, Gq and $G_{12/13}$ (Rosen et al., 2009). The signal that converges from Gi-coupled S1P receptors inhibits the activation of adenylate cyclase and induces the activation of p44/p42 mitogen-activated protein kinase (MAPK). While $S1P_1$ receptor slightly increases intracellular calcium ($[Ca^{2+}]_i$) through $G\beta\gamma$, $S1P_2$ and $S1P_3$ receptors mainly increase $[Ca^{2+}]_i$ through the activation of phospholipase C (PLCβ) from Gq (Watterson et al., 2005). The deletion of $S1P_3$, but not $S1P_2$ receptor in mouse embryonic fibroblasts (MEFs) led to the marked inhibition of S1P-induced PLC activation, which suggests that $S1P_3$ receptor plays an important role in the S1P-induced increase in $[Ca^{2+}]_i$ (Ishii et al., 2002).

$S1P_2$ and $S1P_3$ receptors also couple to $G_{12/13}$ protein to activate a small GTPase, Rho, which is involved in the regulation of actin-cytoskeleton (Ryu et al., 2002; Sugimoto et al., 2003). Rho kinase is activated by Rho through the $G_{12/13}$-Rho guanine nucleotide exchange factor family. S1P-induced Rho activation has been shown to be significantly reduced in $S1P_2$, but not $S1P_3$, receptor-null MEFs (Ishii et al., 2002). Meanwhile, an association between $S1P_3$ receptor and Rho activation has been reported in cells expressing $S1P_3$ receptor (Sugimoto et al., 2003). An S1P-induced contraction of vascular smooth muscle cells has been ascribed to an increase in $[Ca^{2+}]_i$ and Rho activation (Ohmori et al., 2003; Watterson et al., 2005). S1P-induced vasoconstriction is significantly inhibited in cerebral arteries isolated from $S1P_3$ receptor-null mice, but not in those from $S1P_2$ receptor-null mice (Salomone et al., 2008). In addition, Y-27632, a selective Rho kinase inhibitor, inhibits S1P-induced vasoconstriction in canine cerebral arteries (Tosaka et al., 2001), indicating that $S1P_3$ receptor plays an indispensable role in S1P-induced vasoconstriction mediated by Rho-Rho kinase signaling. Although S1P decreases coronary flow (CF) in isolated perfused canine heart, the receptor subtype that is responsible for the S1P-induced reduction of CF has not yet been fully identified. To distinguish $S1P_3$ receptor-dependent signal from $S1P_2$ receptor-dependent signal, a $S1P_3$ receptor-specific antagonist has been needed.

We have developed an $S1P_3$ receptor antagonist, 1-(4-chlorophenylhydrazono)-1-(4-chlorophenylamino)-3,3-dimethyl-2-butanone (TY-52156). By confirming that TY-52156 has a selective antagonistic effect toward $S1P_3$ receptor, we can delineate the role of $S1P_3$ receptor-specific signaling in vascular contraction. Moreover, the effectiveness of TY-52156 in vivo was bolstered by evidence that $S1P_3$ receptor-dependent bradycardia was suppressed by the oral

administration of TY-52156.

Materials and Methods

Materials

TY-52156 was synthesized in our laboratories. Materials were purchased from the following suppliers: S1P from BIOMOL International, L.P. (Plymouth Meeting, PA, USA); SEW2871, FTY-720 and FTY-720 (*S*)-Phosphate from Cayman Chemical (Ann Arbor, MI, USA); VPC23019 from Avanti Polar Lipids, Inc. (Alabaster, AL, USA); JTE013 from Tocris Bioscience (Southampton, UK); U46619 from Calbiochem (Darmstadt, Germany); HuMedia-EG2 and HuMedia-SG2 from Kurabo (Osaka, Japan); and membranes containing human $S1P_1$, $S1P_2$, $S1P_3$, or $S1P_5$ receptors from Millipore (Bedford, MA, USA).

Synthesis of TY-52156

5,5-Dimethyl-2,4-dihexanone (**1**)

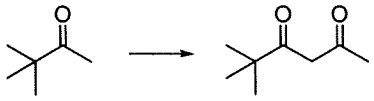

Diisopropyl ether (3 L) was placed in a 5 L 3-neck round-bottom flask and stirred mechanically. Potassium *tert*-butoxide (324 g, 2.25 mol, 1.5 eq) was suspended in the diisopropyl ether at 0 °C. Pinacolone (150 g, 1.50 mol, 1.0 eq) in ethyl acetate (440 mL, 4.50 mol, 3.0 eq) was slowly added dropwise so that the temperature would remain below 10 °C under ice-bath cooling. The reaction mixture was then stirred for 20 h at ambient temperature. Water (1 L) was added slowly so that the temperature would remain below 10 °C under ice-bath cooling. The separated organic layer was extracted with 1N sodium hydroxide (150 mL). The basic aqueous layer was carefully acidified with 6 N HCl (750 mL, 2.0 equivalents of base) at 0 °C and then extracted twice with

petroleum ether (750 mL). The combined organic layer was washed with water (475 mL) and saturated brine (475 mL), dried over anhydrous sodium sulfate, filtered and evaporated at 200 mm Hg and ambient temperature. The remaining liquid was distilled under reduced pressure, with heating up to 80 °C. The title compound (**1**) was obtained as a colorless oil (126 g, 0.89 mol, 59%); ^{1}H-NMR (300 MHz, $CDCl_3$) δ: 1.17 (s, 9 H), 2.08 (s, 3 H), 5.61 (s, 1 H); bp.: 62-69 °C (20 mmHg).

3-Chloro-5,5-dimethyl-2,4-dihexanone (**2**)

5,5-Dimethyl-2,4-dihexanone (**1**) (35.4 g, 249 mmol, 1.0 eq) was dissolved in chloroform (700 mL) and stirred mechanically. Sulfuryl chloride (260 mL, 324 mmol, 1.3 eq) in chloroform (130 mL) was slowly added dropwise so that the temperature would remain below 5 °C under ice-bath cooling. The reaction mixture was then stirred for 2 h at 25 °C, and then quenched with water (500 mL) at 0 °C. The separated organic layer was washed three times with water (500 mL), dried over anhydrous sodium sulfate, filtered and evaporated. The residue was purified by distillation under reduced pressure, with heating to 70 °C. The title compound (**2**) was obtained as a yellow oil (41.5 g, 235 mmol, 94%); ^{1}H-NMR (300 MHz, $CDCl_3$) δ: 1.23 (s, 9 H), 2.38 (s, 3 H), 5.09 (s, 1 H); bp.: 67-69 °C (1.5 mmHg).

[1-Chloro-1-(4-chlorophenylhydrazono)]-3,3-dimethyl-2-butanone (**3**)

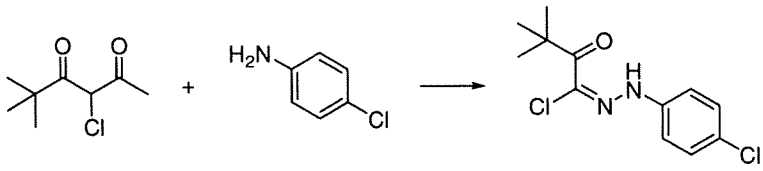

4-Chloroaniline (29 g, 226 mmol, 1.0 eq) was added to 6 N hydrochloric acid (158 mL, 951 mmol, 4.2 eq) and water (68 mL) and stirred for 15 min at 0 °C. Sodium nitrite (17 g, 249 mmol, 1.1 eq) in water (90 mL) was slowly added dropwise so that the temperature would remain below 5 °C under ice-bath cooling. The reaction mixture was stirred for 1 h at 0 °C to prepare a solution of diazonium salt. 3-Chloro-5,5-dimethyl-2,4-dihexanone (**2**) (40 g, 226 mmol, 1.0 eq) was dissolved in pyridine (158 ml) and water (158 mL) at 0 °C. The previously prepared diazonium salt solution was slowly added dropwise so that the temperature would remain below 10 °C, and the resulting mixture was then vigorously stirred for 2 h, with warming from 0 to 25 °C. The reaction mixture was extracted with ethyl acetate (452 mL), washed twice with 2N HCl (1 L) and saturated brine (452 mL), dried over anhydrous sodium sulfate, filtered and evaporated. The resulting crude product was diluted with methanol (226 ml, 1M solution), refluxed for 1 h and then cooled to 0 °C. The precipitated crude crystals were collected by filtration, washed with petroleum ether, and dried under reduced pressure to give the title compound (**3**) as a yellow solid (24 g, 89 mmol, 39%); ^{1}H-NMR (300 MHz, $CDCl_3$) δ: 1.43 (s, 9H), 7.12 (d, J = 8.7 Hz, 2H), 7.33 (d, J = 8.7 Hz, 2H), 8.34 (s, 1H); m.p.: 129-131 °C.

2-(4-Chlorophenylhydrazono)-2-(4-chlorophenylamino)acetophenone (**TY-52156**)

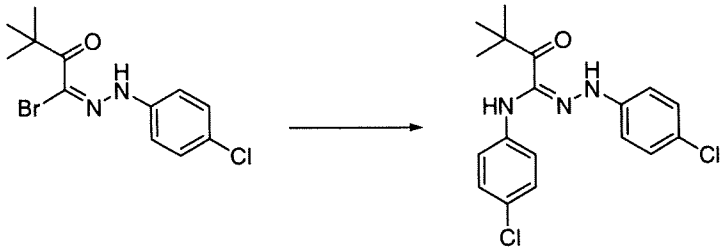

[1-Chloro-1-(4-chlorophenylhydrazono)]-3,3-dimethyl-2-butanone (**3**) (22.4 g, 82.1 mmol, 1.0 eq) and 4-chloroaniline (11.5 g, 90.4 mmol, 1.1 eq) were dissolved in ethanol (274 mL), and triethylamine (13.7 mL, 98.6 mmol, 1.2 eq) was then added at 0 °C. The resulting mixture was stirred for 3 h at ambient temperature. The reaction mixture was evaporated, quenched with water (82 mL), and diluted with ethyl acetate (165 mL). The organic layer was washed with water (165 mL) and saturated brine (165 mL), dried over anhydrous sodium sulfate, filtered and evaporated. The resulting crude crystals were washed with a solvent mixture of hexane-ethyl acetate (20:1) and dried under reduced pressure to obtain the title compound (**TY-52156**) as a yellow powder (24.8 g, 68.1 mmol, 83%); ^{1}H-NMR (300 MHz, $CDCl_3$) δ: 1.48 (s, 9H), 6.55 (d, J = 8.4 Hz, 2H), 6.76 (s, 1H), 6.98 (d, J = 8.8 Hz, 2H), 7.19-7.26 (m, 5H); MS (ESI) m/z = 362 $(M-H)^-$; mp.: 90-91 °C.

Cell Culture

Chinese hamster ovary (CHO-K1) cells that stably expressed human $S1P_1$ ($S1P_1$-CHO), $S1P_2$ ($S1P_2$-CHO) or $S1P_3$ ($S1P_3$-CHO) receptors were maintained as described previously (Koide et al., 2007). A human recombinant $S1P_4$ receptor-expressing cell line ($S1P_4$-Chem) was purchased from Millipore. Human umbilical vein endothelial cells (HUVECs) purchased from DS Pharma Biomedical (Osaka, Japan) were cultured on collagen-coated dishes in HuMedia-EG2. Human coronary artery smooth muscle

cells (HCASMCs) purchased from Kurabo were cultured in HuMedia-SG2.

Measurement of the Intracellular Calcium Concentration

$[Ca^{2+}]_i$ in $S1P_1$-, $S1P_2$-, $S1P_3$-CHO, and $S1P_4$-Chem was measured using the calcium-sensitive dye Fura-2 AM, as described previously (Koide et al., 2007). The fluorescence (excitation at 340 and 380 nm; emission at 510 nm) was measured with a FLEXStation II (Molecular Devises). The ratio of the fluorescence intensity at two wavelengths (FR340/380) was calculated. The *K*i value for TY-52156 was estimated from Ca^{2+} responses as described previously (Ohta et al., 2003).

[^{3}H]-S1P Binding Assay

A [^{3}H]-S1P binding assay was performed as described by Lim et al. (2003) with minor modifications. The cell membrane (60 μg/mL) was incubated with binding buffer containing [^{3}H]-S1P (1 nM, about 40,000 dpm per well) and vehicle or each concentration of TY-52156 (μM) for 30 min at 25°C. Radioactivity was measured by a liquid scintillation counter after the addition of scintillation cocktail solution. Nonspecific binding was defined as the amount of radioactivity bound to the cells in the presence of unlabeled S1P (3.0 μM). Specific binding was calculated by subtracting nonspecific binding from total binding.

GTP-binding Assay

Europium-GTP (Eu-GTP) binding was determined using a DELFIA GTP Binding Assay Kit (Perkin-Elmer Life Sciences, Wallac, Turku, Finland). Samples were incubated in AcroWell filter plates (PALL, Ann Arbor, MI, USA) for 60 min ($S1P_1$ and $S1P_5$) or 90

min ($S1P_2$ and $S1P_3$) at 30°C. The reaction was started by adding membranes (48 μg/mL) containing human $S1P_1$, $S1P_2$, $S1P_3$ or $S1P_5$ receptors to the assay buffer (20 mM HEPES, pH7.4, 5 mM $MgCl_2$, 100 mM NaCl, 1.2 mg/mL Saponin, 10 μM GDP and 10 nM Eu-GTP at 30°C) including S1P (0.1 μM) and vehicle or the desired concentration (μM) of the test drug (TY-52156 or VPC23019). The reaction was terminated by rapid filtration and the filter was washed five times with 200 μL of ice-cold washing solution in a vacuum manifold. The plate was measured by time-resolved fluorescence (340 nm excitation/615 nm emission) using a EnVision (Perkin-Elmer Life Sciences).

Western Blot Analysis for p44/p42 MAPK

$S1P_1$-, $S1P_2$- and $S1P_3$-CHO (2.0×10^5 cells) were plated on 6-well plates and cultured with Nutrient Mixture F-12 Ham (Sigma) containing 1% FBS for 4 h before the experiments. The cells were treated with vehicle, TY-52156 (TY) (10 μM), VPC23019 (VPC) (10 μM) or JTE013 (JTE) (1.0 μM) for 10 min and then with vehicle or S1P (0.1 μM) for 5 min at 37°C. The cells were lysed in CelLyticM containing Protease Inhibitor Cocktails and Phosphatase Inhibitor Cocktails (Sigma) for 10 min at 4°C. The lysate was centrifuged at 13,000×g for 15 min at 4°C and supernatant was transferred to a fresh tube. The protein concentration was determined using the Bradford method. Equal amounts of proteins were resuspended in 4×Sample Buffer (Wako Pure Chemical Industries), boiled for 5 min and separated by 10% SDS-PAGE. After being transferred to a polyvinylidene fluoride (PVDF) membrane, the membranes were blocked in Block Ace (DS Pharma Biomedical) and immunoblotted with antibodies of phospho-p44/p42 MAPK or p44/p42 MAPK (1:1000, Cell Signaling

Technology). The signals were visualized by an Amplified Alkaline Phosphatase Goat Anti-Rabbit Immun-Blot Assay Kit (Bio-Rad) according to the manufacturer's instructions. Quantitative analyses of immunoblots were performed using Quantity One version 4.2.2 software (Bio-Rad). The relative percentage compared with the vehicle was calculated and expressed as the mean±S.E.M.

Measurement of Coronary Flow

All animal experiments were reviewed and approved by the Experimental Animal Committee in our laboratories. Male Sprague–Dawley (SD) rats (300-350 g; Nihon SLC) were anesthetized by the injection of pentobarbital (50 mg/kg i.p.). After thoracotomy, their hearts were rapidly excised and perfused at 37°C in a Langendorff manner with Krebs-Henseleit bicarbonate buffer (constant perfusion pressure of 70±5 mmHg) of the following composition (in mM): NaCl 118; KCl 4.7; KH_2PO_4 1.2; $MgSO_4$ 1.2; $CaCl_2$ 2.5; $NaHCO_3$ 24.9; EDTA/2Na 0.027; ascorbic acid 0.057 and glucose 11.1, pH 7.4 at 37°C, bubbled with 95% O_2 and 5% CO_2 (pO_2>550 mmHg). A modified water-filled latex balloon (LB-2, Technical Service Corporation) was inserted into the left ventricle via the left atrium with a pressure transducer (DX-360, Ohmeda) connected to an amplifier (AP-601G, Nihon Kohden). Left ventricular end-diastolic pressure was adjusted to about 5-10 mmHg. To measure coronary flow (CF), a Cannulating-type Flow Probe (FF-030T, Nihon Kohden) connected to an electro-magnetic blood-flow meter (MFV-3700, Nihon Kohden) was inserted to the perfusion line that was connected to the heart. After a 15-min period for equilibration, vehicle, TY-52156 (TY) (0.1 μM), VPC23019 (VPC) (0.1 μM) or JTE013 (JTE) (0.1 μM) was infused for 10 min by an infusion pump (Harvard Apparatus) through a

drug-infusion line connected to the main perfusion line at a flow rate of 1/100 the CF rate. After drug treatment, vehicle or the indicated concentration of S1P (μM) or U46619 (0.1 μM) was added to the same line. CF was measured before and 10 min after the infusion of S1P or U46619. The relative percentage compared to the vehicle was calculated from the CF rate.

Contractile Response in Cerebral Arteries

Beagle dogs (Oriental Yeast) were anesthetized by the injection of pentobarbital (30 mg/kg i.p.). The cerebral arteries were rapidly excised and mounted in organ chambers containing Krebs buffer of the following composition (in mM): NaCl 118.0, KCl 4.7, $CaCl_2$ 2.5, KH_2PO_4 1.2, $MgSO_4$ 1.2, $NaHCO_3$ 25.0 and glucose 11.0, pH 7.2 at 37°C, bubbled with 95% O_2 and 5% CO_2. After equilibration, cerebral arteries were exposed to 60 mM KCl until the contractile responses were stabilized. After washout and recovery, contractile responses to S1P were measured every 10 min after the addition of the indicated concentration of S1P (μM). In another experiment, the cerebral arteries were contracted by S1P (5.0 μM), and then an increasing amount of vehicle or TY-52156 (up to 10 μM) was applied to the organ chambers. Relaxation responses were measured every 10 min after addition of the indicated concentration of vehicle or TY-52156 (μM). The degree of contraction compared to vehicle was calculated with PRISM version 4 statistical software (GraphPad) and expressed as the percent contraction compared to that induced by S1P.

Immunoprecipitation and Western Blot

HCASMCs were seeded at 5×10^5 cells in a culture dish. After they reached